Fracture mesomechanics of a solid as a nonlinear hierarchically organized system

V.E. Panin

Institute of Strength Physics and Materials Science SB RAS, Tomsk, 634021, Russia

paninve@ispms.tsc.ru

Keywords: fracture, nonlinear mesomechanics, hierarchical system.

Abstract. Any loaded solid is a multiscale nonlinear system consisting of two subsystems: a planar subsystem (surface layers and all kinds of interfaces, including shear bands) and a crystalline one. Self-consistent plastic flow within the two subsystems is realized by nonlinear waves of local structural transformations. Fracture of a solid develops as its structure-phase decomposition in a nonlinear wave of localized plastic flow characterized by a positive Gibbs thermodynamic potential.

Introduction

Classical fracture mechanics is based on a linear approach and treats fracture as a single-scale process [1]. In the last two decades, a multiscale approach to description of fracture has been intensively developed [2]. In so doing, the main challenge lies in self-consistent description covering the contiguous scales: pico–nano, nano–micro, and micro–macro, and this comes to the scope of mesomechanics [3].

Physical mesomechanics uses a unified multiscale approach to describe plastic deformation and fracture of solids as nonlinear hierarchically organized systems [4, 5]. The approach rests on the concept of structural scales of deformation and nonequilibrium thermodynamics of structural or structural phase transformations under highly nonequilibrium conditions. This multiscale approach is followed in the work to provide self-consistent description of fracture in a loaded hierarchically organized system.

1. Fracture as local structure-phase decomposition of a nonequilibrium crystalline state.

Physical mesomechanics, as applied to structural scales of plastic deformation and fracture, classified two types of subsystems: a planar subsystem free of translation invariance (surface layers, internal interfaces, macrobands of localized deformation) and a translationally invariant crystalline subsystem of any scale. The fundamental difference of these two subsystems is in their thermodynamic state which can be expressed in terms of the Gibbs thermodynamic potential:

$$F(v) = u - ST + pv - \sum_{i=1}^{N} \mu_i c_i, \qquad (1)$$

where u is internal energy, S is entropy, T is temperature, p is pressure, v is the molar volume, μ_i is the chemical potential of an element of concentration c_i. From (1) it follows that as the level of F in a deformed solid increases due to the terms u and pv, local minima of its metastable states can arise in response to entropy production and redistribution of dopants (or impurities). These effects are represented by the $F = F(v)$ curve, where the molar volume v is considered as a generalized thermodynamic parameter (Fig. 1). The expression for the entropy production σ_s has the form [5]:

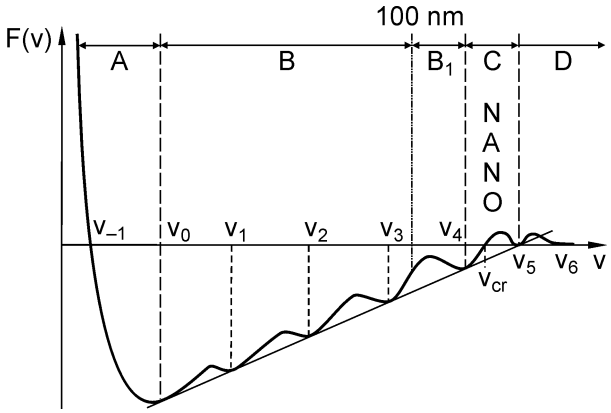

Fig. 1. Dependence of the Gibbs thermodynamic potential on the molar volume, $F(v)$, accounting for local hydrostatic compression region A and hydrostatic tension regions at different scales where defect structures are generated: B is mesoscale substructures of different structural scales, B_1 is the nanosized structures, C is the nanostructural states and D is the ensuing porosity and fracture regions.

$$\sigma_s = \frac{\kappa(\nabla T)^2}{T^2} + \rho\frac{\boldsymbol{\nu\sigma}}{T} \pm \frac{\rho}{T^2}([\boldsymbol{\alpha\nu}], \nabla T), \qquad (2)$$

where κ is the heat conductivity, ρ is the material density, $\boldsymbol{\nu}$ is proportional to the defect flux density, $\boldsymbol{\sigma}$ is the local stress in the zone of defect phase nucleation, $\boldsymbol{\alpha}$ is defect density.

The first term in (2) is the entropy production due to heat release. The second term determines the work of a defect flow as it moves in the stress field. The third term relates to the mechanical field energy flux in a crystal through the surface bounding the zone of local structural transformation during the formation of a defect phase.

The first two terms are always positive and responsible for an increase in entropy. The third term can be both positive and negative. As metastable defect phases arise in a crystal, self-ordering in its local distortion zone occurs and entropy decreases. This reflects relaxation of mechanical field disturbance in the deformed crystal in response to local structural transformation arising in a local hydrostatic tension zone. Under these conditions, the third term in expression (2) goes negative and lowers the overall increase in entropy during the formation of a defect substructure.

However, as a crack nucleates and propagates in a loaded crystal, the zone of hydrostatic tension and local distortion at the crack tip always survives. Mechanical field relaxation in this zone occurs through crack propagation with attendant multiscale fragmentation of the material and increase in entropy. The third term in (2) thus goes positive. Hence, if a crack develops in a deformed crystal, all three terms in (2) are found positive. This is responsible for fracture irreversibility[1].

According to [4, 5], primary shear in a loaded crystal develops in its planar subsystem as nonlinear waves of local structural transformations. The thus arising local compaction regions of the material experience structural transformations and are periodically injected into the crystalline subsystem as dislocation cores (or other types of strain-induced defects). The latter provide plastic form changing in the crystalline subsystem. This process is qualified as a nonlinear wave of local structural transformations and the strain-induced defects involved in are called an inhibitor.

[1] The effects of microcrack healing known in the literature are thermodynamically possible in specific nanostructural states. This issue is not considered here.

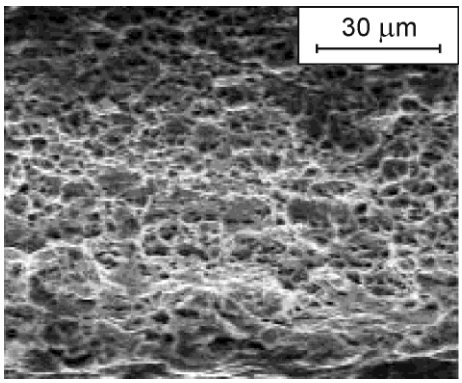

Fig. 2. Porous nanostructure on the fracture surface of composite alloy Cu – 25 % Cr.

An increase in the molar volume v of a deformed solid gives rise to dislocations, shear bands, deformation twins, disclinations, meso- and macrobands of localized deformation which determine the mechanisms of plastic deformation in its crystalline subsystem.

Finally, at $v > v_{cr}$ when $F(v)$ becomes positive, the crystal loses its thermodynamic stability in local zones of highly nonequilibrium states and experiences structure-phase decomposition. Atoms of the decomposed crystalline zone complete the walls of the surrounding crystal, and the excess molar volume in these zones gives rise to cracks or pores. It is seen from Fig. 1 that the formation of a crack is preceded by the formation of a two-phase nanostructural zone at molar volumes $v_4 \div v_5$ [6]. In this two-phase nanostructural state, according to [6], nanocrystals with $F(v) < 0$ and an amorphous phase with $F(v) > 0$ coexist. As the molar volume further increases, pores arise in the amorphous phase, being indicative of the onset of structure-phase decomposition of the crystalline state. This process plays a fundamentally important role in crack nucleation and propagation. Allowance for nonequilibrium thermodynamics qualitatively changes the existing paradigm of linear fracture mechanics. In nonlinear physical mesomechanics, it is generally taken that any kind of fracture develops in zones of nanostructural states in which pores are surrounded by nanostructured walls (Fig. 2). In other words, the nucleation and propagation of a crack should be described as local thermodynamic structure-phase decomposition of nanostructural states in nonequilibrium zones. The mesomechanics of the formation of these porous nanostructures is considered below.

2. Experimental basis for mesomechanics of structure-phase decomposition of a solid ahead of the crack tip

Hierarchical self-consistency of structural scales of plastic deformation and fracture was studied most comprehensively in the neck of tensile metal specimens [7–9]. Schematic of the multiscale stress-strain state is shown in Fig. 3 [7, 8]. Strain localization in the neck owes to two localized plastic flow macrobands *AB* and *CD* developed in the neck self-consistently by the cross pattern.

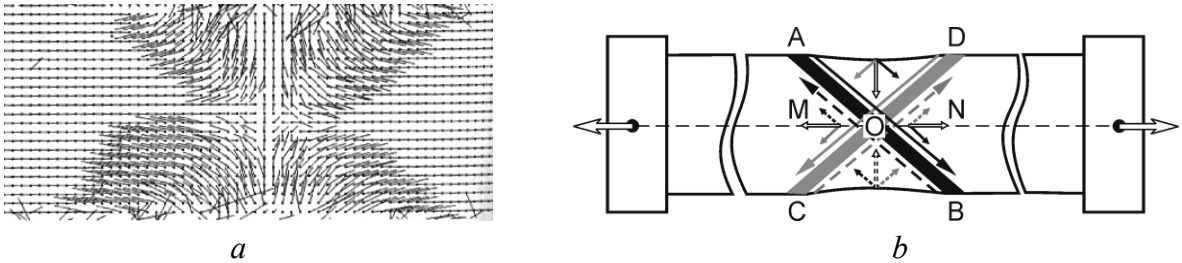

a *b*

Fig. 3. Displacement vector field in the neck (*a*) and schematic representation of shear self-consistency at the interaction of localized deformation macrobands self-organized by the cross pattern (*b*) [7].

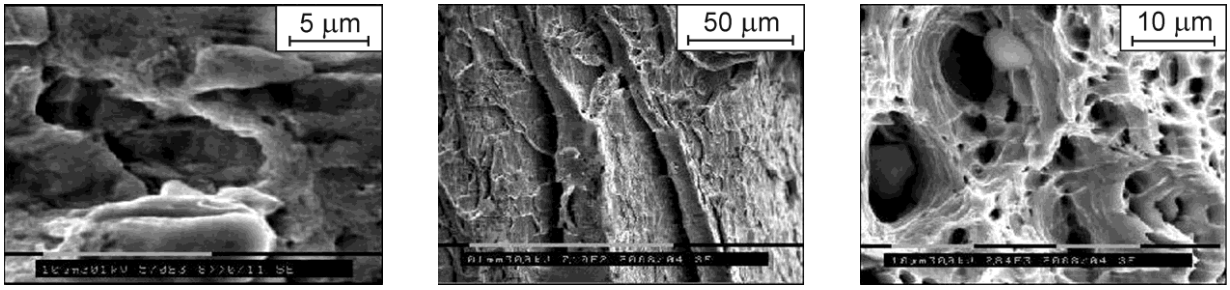

a *b* *c*

Fig. 4. Structure of the fracture surface of the submicrocrystalline α-Fe specimen [8].

The vector sum of localized shear strains in the macrobands *AB* and *CD* governs uniaxial tension of the material in the neck centre (vectors *OM* and *ON*) and its transverse compression in trihedral prisms *AOD* and *COB* (Fig. 3(*b*)). Experimental displacement vector fields (Fig. 3(*a*)) reveal vortex plastic flow in the zones *AOD* and *COB* with attendant mesoscale fragmentation of the material [10]. Strain hardening of the fragmented material retards its transverse shear toward the neck centre. At a certain plastic strain degree, transverse shear is completely blocked, and a hydrostatic tension zone arises in the neck centre. In this zone, a porous nanostructure is formed (Fig. 4(*c*)), [8] in which an opening mode crack nucleates. At the first stage, the main crack propagates crosswise the specimen, reducing its cross-section and decreasing the applied stress. As the specimen cross-section decreases to a certain value, the opening mode crack is first transformed into a sliding mode crack (Fig. 4(*b*)) and then into a tearing mode crack (Fig. 4(*a*)).

At the first stage of tension of submicrocrystalline titanium [11], an inclined neck arose in which one macroband of localized deformation developed rapidly in the direction of maximum tangential stress τ_{max}. Measurements of the strain components ε_{xy}, ε_x and ε_y in the macroband revealed that both the shear and linear components in the shear macroband progressively increase. The process culminates in the development of a tearing mode crack in the macroband. Scanning electron microscopy and laser profilometry disclose wave development of roughness on fracture surface which characterizes fracture toughness. Physical mesomechanics allows description of the wave nature of crack propagation in a multiscale solid in fracture.

3. Nonlinear waves of localized plastic deformation and fracture. According to the theory of elasticity, an inhomogeneous stress-strain state arises at the crack tip in which all stress concentration zones in conjugate directions of maximum tangential stress are clearly defined (Fig. 5) [12].

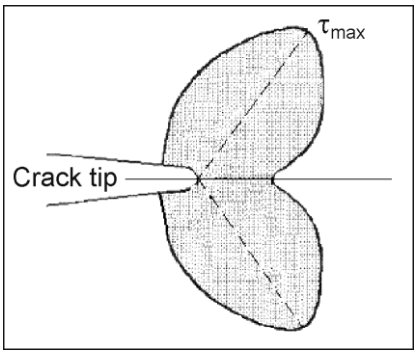

Fig. 5. A scheme of stress distribution ahead of a notch or crack tip [12].

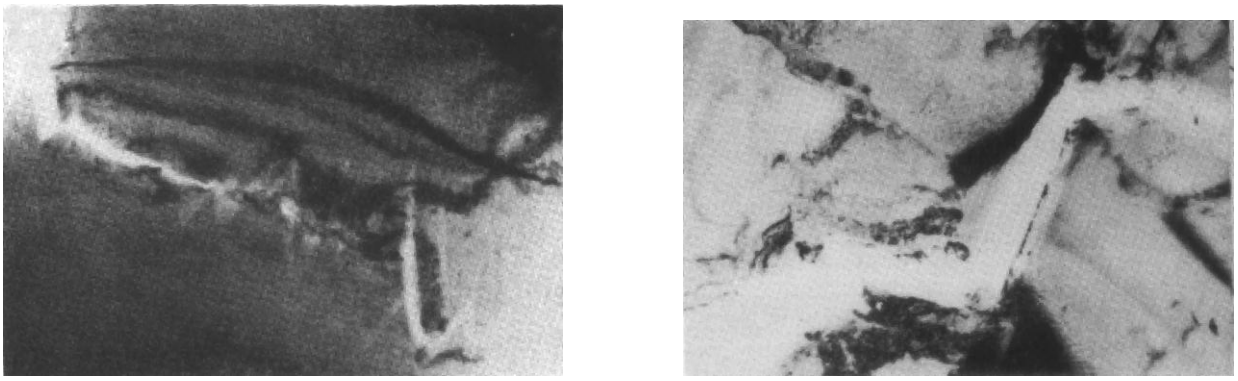

a *b*

Fig. 6. Tension in situ of austenitic steel: *a* — development of a localized zigzag mesoband ahead of the crack tip, ×1 500; *b* — propagation of a zigzag crack along mesoband, ×1 200; high-voltage TEM [13].

Experiment shows that in these directions ahead of the crack tip, zigzag plastic shear displacements develop, dictating the trajectory of subsequent crack propagation (Fig. 6) [13]. This underlies the nonlinear wave nature of channeled crack propagation along mesobands of localized plastic deformation [14]. The physical mesomechanics of these nonlinear waves gives an insight into channeled plastic shear [15, 16]. However, if the molar volume in the zone of wave plastic shear exceeds the critical value v_{cr} at which the Gibbs thermodynamic potential becomes positive, the wave plastic shear is followed by a nonlinear fracture wave.

Let us demonstrate this with the wave theory of channeled plastic shear [15, 16].

A special case of the wave equations derived in [15, 16] are the equations for non-dimensional linear defect flux ***J*** and density $\boldsymbol{\alpha}$ (discontinuities of the displacement vector **u**):

$$\frac{\partial}{\partial x_\alpha} J_\mu^\alpha = -\frac{\partial \ln u_\mu}{\partial t}, \tag{3}$$

$$\varepsilon_{\mu\chi\delta}\frac{\partial J_\delta^\alpha}{\partial x_\chi} = -\frac{\partial \alpha_\mu^\alpha}{\partial t}, \tag{4}$$

$$\frac{\partial \alpha_\mu^\alpha}{\partial x_\alpha} = 0, \tag{5}$$

$$\varepsilon_{\mu\chi\delta}\frac{\partial \alpha_\delta^\alpha}{\partial x_\chi} = \frac{1}{\tilde{c}^2}\frac{\partial J_\mu^\alpha}{\partial t} + \sigma_\mu^\alpha - P_\mu^\beta \frac{C_{\alpha\beta}^{\mu\nu}}{E}, \tag{6}$$

$$\frac{1}{c^2}\frac{\partial \nu_\mu}{\partial t} = \frac{\partial \sigma_\mu^\alpha}{\partial x_\alpha} - \frac{\partial P_\nu^\beta C_{\alpha\beta}^{\mu\nu}}{\partial x_\alpha E}, \tag{7}$$

where $\nu_\mu = \dfrac{\partial \ln u_\mu}{\partial t}$ is the elastic strain rate in a defect medium, $\sigma_\mu^\alpha = \dfrac{\partial \ln u_\nu}{\partial x_\beta}\dfrac{C_{\alpha\beta}^{\mu\nu}}{E}$ is the elastic stresses in the defect medium, c and $\tilde{c}$ are the velocity of sound and the plastic front perturbation velocity, $P_\mu^\beta(x,t)$ is the plastic part of distortion, $\varepsilon_{\mu\chi\delta}$ is the Levy-Civita symbol, and $C_{\alpha\beta}^{\mu\nu}$ is elastic constants.

Equations (3)–(7) have the following meaning. Equation (3) is the continuity equation for a defect medium from which it follows that the plastic flow source is the defect rearrangement rate. Equation (4) is the plastic strain compatibility condition. Of critical importance is that temporal variations in the medium density, in this case, are determined not by the divergence but by the curl rot of the defect flux, i.e., by its spatial inhomogeneity. Equation (5) is the defect continuity condition which accounts for the absence of charges of the vortex component of the plastic strain field $(\alpha_\chi^\beta = \varepsilon_{\chi\mu\nu}\partial_\mu P_\nu^\beta)$. Equation (6) is the constitutive relation for a medium undergoing plastic deformation. Equation (7) is the well-known quasi-elastic equilibrium equation used in continuum mechanics, with the right-hand side of (7) incorporating plastic distortions in addition to elastic strain. In effect, this term accounts for nucleation of strain-induced defects in local hydrostatic tension regions generated by a stress concentrator.

Equation (6) is valid for a medium subjected to plastic deformation and relates temporal variations of the plastic flow with anisotropic spatial variations of the defect density $(\varepsilon_{\mu\chi\delta}\partial\alpha_\delta^\alpha/\partial x_\chi)$ and with the source $(\sigma_\mu^\alpha - P_\nu^\beta C_{\alpha\beta}^{\mu\nu}/E)$. The difference of Eqs. (6), (7) from pertinent equations of the theory of elasticity is that temporal variations of the plastic strain rate are governed by the stresses involved rather than by $\partial\sigma_\mu^\alpha/\partial x$, as in the elastic case. Moreover, the plastic distortion $P_\nu^\beta(x,t)$ enters into the right-hand side of Eq. (6) as defect sources. This is evidence of a dual nature of defects as field sources.

The wave equations for the non-dimensional defect fluxes ***J*** and density $\boldsymbol{\alpha}$ can be derived from the system of equations (3)–(7). Thus,

$$\frac{1}{c^2}\frac{\partial^2 J_\alpha^\mu}{\partial t^2} - \frac{\partial^2 J_\alpha^\mu}{\partial x_\nu^2} = \frac{\partial}{\partial t}\left\{\frac{\partial \ln u_\alpha(x,l)}{\partial x_\mu} - \frac{1}{E}\frac{\partial \ln u_\beta}{\partial x_\nu}C_{\alpha\beta}^{\mu\nu} - \frac{1}{E}P_\nu^\beta C_{\alpha\beta}^{\mu\nu}\right\}, \tag{8}$$

$$\frac{1}{c^2}\frac{\partial^2 \alpha_\alpha^\mu}{\partial t^2} - \frac{\partial^2 \alpha_\alpha^\mu}{\partial x_\nu^2} = \varepsilon_{\mu\chi\sigma}\left\{\frac{\partial^2 \ln u_\beta(x,t)}{\partial x_\chi \partial x_\nu}C_{\alpha\beta}^{\mu\nu} - \frac{\partial P_\nu^\beta}{\partial x_\chi}C_{\alpha\beta}^{\mu\nu}\right\}\frac{1}{E} \tag{9}$$

with the proviso that the sources are compatible:

$$\frac{\partial N_\mu}{\partial t} + \varepsilon_{\mu lm}\frac{\partial M_m}{\partial x_l} = 0. \tag{10}$$

Here *M* is the right-hand side of Eq. (8), *N* is the right-hand side of Eq. (9), and ***u***(*x*, *t*) is the inelastic displacements within the wave of inelastic localized deformation.

The right-hand side of Eq. (8) describes the defect flux sources determined by the quasi-elastic strain rate $\frac{\partial}{\partial t}(E_\mu^\alpha E - E_\nu^\beta C_{\alpha\beta}^{\mu\nu})\frac{1}{E}$. The bracketed expression is the difference in values between internal compressive (tensile) and shear stresses associated with stress distribution in the stress concentrator region. The relaxation of defect rearrangement (to form clusters of different atomic configurations or their conglomerates) is represented by the term $P_\nu^\beta C_{\alpha\beta}^{\mu\nu}/E$ in Eq. (8). The right-hand side of Eq. (9) describes a strain-induced defect density source produced by the shear strain vorticity $\varepsilon_{\mu\chi\delta}\frac{\partial}{\partial x}(E_\nu^\beta - P_\nu^\beta)\frac{C_{\alpha\beta}^{\mu\nu}}{E}$ due to shear stress relaxation in local hydrostatic tension regions.

The wave pattern of the strain-induced defect flow is determined by the right-hand side of Eqs. (8) and (9). The plastic distortion $P_{\nu}^{\beta}(x,t)$ plays a crucial role in the wave propagation of plastic strain.

Before proceeding to wave interpretation of Eqs. (3)–(9), we should emphasize that although wave equations of plastic flow of solids were derived earlier in [17, 18], they were not considered as plasticity waves. A conclusion on wave propagation of elastic-plastic perturbation in a medium is always reasoned from the problem of perturbation group velocity. With no group velocity dispersion, the wave is well defined. The medium inhomogeneity gives rise to wave packet dispersion and breakup. Hence, in the context of the single-scale approach the existence of plasticity waves is beyond question. However, if we consider a deformed solid as a multiscale system, taking into account the "shear plus rotation" pattern of plastic deformation and possibility of channeled local structural transformations, the conclusion on nonlinear plasticity and failure waves is justified. What is more, stress concentrators in plastic shear propagation as local structural transformations are impossible to reproduce without using the nonlinear wave pattern. It is no accident that all known wave equations of plastic flow are similar to equations of electrodynamics and provide a qualitatively similar field behavior [19].

From the foregoing discussion it follows that the source of the strain-induced defect density is the shear strain vorticity $\varepsilon_{\mu\chi\delta}\frac{\partial}{\partial x}(E_{\nu}^{\beta}-P_{\nu}^{\beta})\frac{C_{\alpha\beta}^{\mu\nu}}{E}$ induced by local structural transformations in the quasi-elastic stress concentrator region. The local structural transformations provide relaxation of both oppositely directed shear stresses and hydrostatic tensile stresses in the vicinity of stress concentrators. On completion of local relaxation, the new stress concentrators arises in the applied stress field. The wave process can be expressed analytically for channeled localized deformation under specified boundary conditions.

If we put that the plastic distortion P_{ν}^{β} is equal to zero, equation (8) describes a nonlinear wave of crack propagation. In this case, inelastic shear displacements in a hydrostatic tension zone at the crack tip increase the molar volume, and with the proviso that $v > v_{\mathrm{cr}}$, structural phase decomposition of material ahead of the crack tip takes place, thus providing propagation of a nonlinear fracture wave.

Let us consider a channeled defect flow within a mesoband of localized shear along the direction L. The general coordinate system is chosen such that the Z axis is directed along L, whereas the x and y coordinates vary within the deformed layer thickness. According to [15, 16], the plastic flow distribution in the local region ($r < L$) has the form:

$$\mathbf{J}=\frac{b_1-b_2}{4\pi}\chi(s,t)\mathbf{b}(s,t_n)(\ln\frac{2L}{r}-1)-\nabla f, \qquad (11)$$

where **b** is the binormal vector in the local coordinate system, χ is the variation of curvature of the plastic strain region (axial curvature of the region) due to applied load, t_n is the tangent, s is the running length of the region, b_1 and b_2 are the «Burgers vector» magnitudes of bulk translation and subsurface or rotation incompatibility, respectively, and ∇f is the gradient part of the flow due to external sources.

Let us define variations in the configuration of localized deformation flow of length L and initial size δ. The spatial-temporal variations of the configuration $\mathbf{E}(s, t)$ under deformation can be determined from the following equation:

$$\mathbf{J} = \frac{\partial \mathbf{E}(x,t)}{\partial t}. \tag{12}$$

The expression for **J** and the substitution $t' \to t\ \frac{b_1 - b_2}{4\pi}\left(\ln\frac{2L}{r} - 1\right)$ gives

$$\frac{\partial \mathbf{E}(s,t)}{\partial t} = \chi \mathbf{b} - \frac{4\pi}{(b_1 - b_2)(\ln(2L/r) - 1)}\nabla f. \tag{13}$$

From Eq. (13) it follows that at a high plastic flow velocity, the vorticity of plastic flow characterized by its curvature χ plays a decisive role in deformation, whereas at a low plastic flow velocity, the gradient term in Eq. (13) is of crucial importance. Because high local curvature causes a considerable increase in internal crystal energy, the mesoband is fragmented, and at $v > v_{cr}$, structure-phase decomposition takes place within the highly nonequilibrium defect flow.

It can be shown that high velocity and curvature of a constrained defect flow results in a high molar volume, which is a necessary condition for fracture development.

Let us estimate the physical width 2δ of a deformation region covered by the constrained defect flux *J*. From Eq. (11) it follows that for ***J*** = 0,

$$\delta \cong L\exp\left[-\frac{4\pi(\nabla f \mathbf{b})}{\chi(b_1 - b_2)}\right]. \tag{14}$$

Equation (14) makes clear that the width of the constrained defect flow increases with increasing its curvature χ. Thus, channeled wave defect flows with high curvature are bound to cause propagation of nonlinear fracture waves associated with local structure-phase decomposition of material.

The channeled spiral pattern of localized defect flow with varying curvature χ is illustrated in Fig. 7. It is seen from Fig. 7(*a*) that with a small curvature χ, the transverse strain rate v is low, and the spiral experiences slight torsion characterized by a large transverse wave length. This situation corresponds to the development of plastic shear in highly nonequilibrium surface layers, interfaces and shear bands. As the curvature increases, the transverse wave length decreases greatly, whereas the transverse strain rate increases (Fig. 7(*b*)). With high curvature χ, hydrostatic tension and structure-phase decomposition of material develop in these regions, giving rise to cracking.

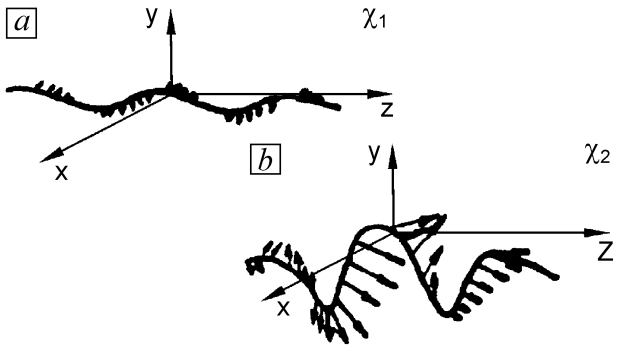

Fig. 7. Localized plastic deformation configuration and velocity as a function of the curvature χ of the deformed region: $\chi_1 < \chi_2$ [16].

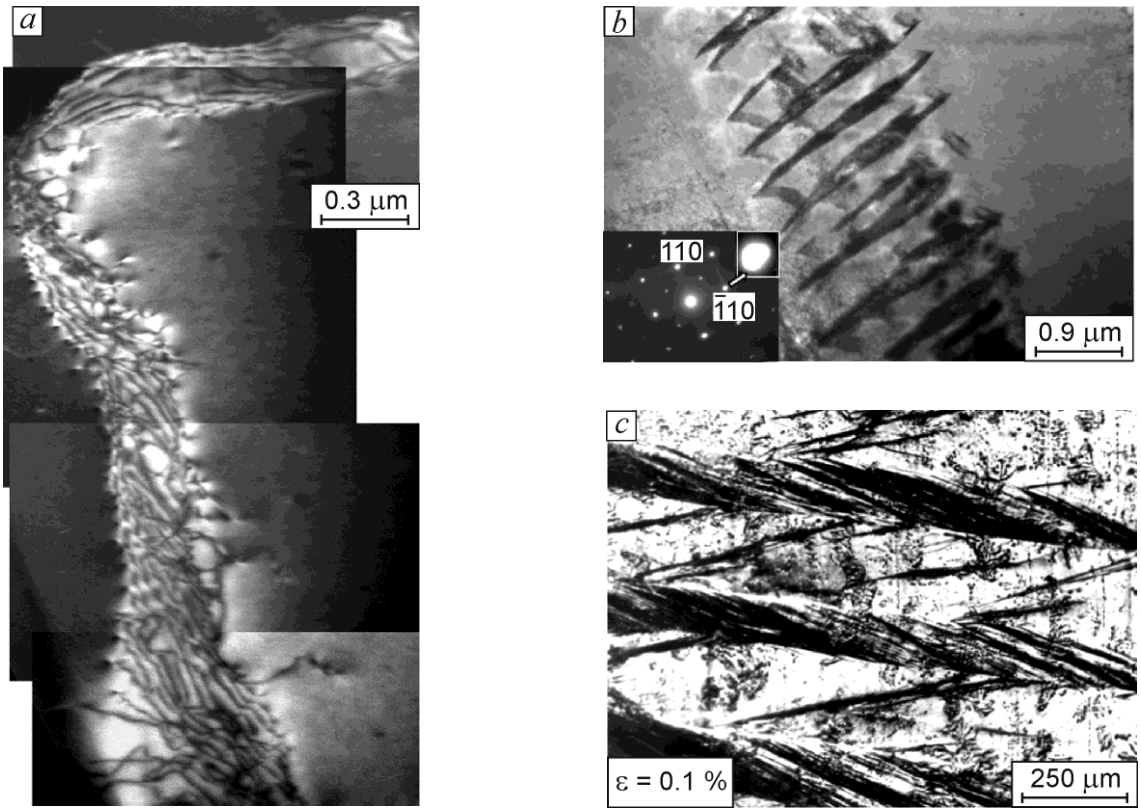

Fig. 8. Spiral nonlinear wave flow as local structure-phase decomposition in aluminum foil, alternate bending, $N = 4 \cdot 10^5$ cycles, $T = 293$ K [21] (*a*); lamella of B19′ martensite within nonlinear wave of localized shear in B2 austenite single crystal TiNi (Fe, Mo), tension, $T = 773$K; TEM [23] (*b*); spiral nonlinear wave shear on the surface of [001]- single crystal TiNi (Fe), compression, $T = 573$ K, light mycroscopy [23] (*c*).

Experimental studies of mesobands of localized deformation propagating as spirals are reported in [21–23]. Examples of these spiral mesobands are given in Fig. 8. The spiral mesobands are readily observable in plastic deformation of highly nonequilibrium materials with low shear stability. Figure 8(*a*) shows a spiral mesoband formed in Al foil in alternate bending after $N = 4 \cdot 10^5$ cycles [21]. Plastic deformation in compressed NiTi single crystals can proceed either through thermoelastic martensite transformation B2–B19′ (Fig. 8(*b*)) or through microtwinning (Fig. 8(*c*)) with attendant development of spiral mesobands whose form depends on their formation mechanism. This issue is considered at greater length in [21–23].

4. Effect of the structure-phase state and loading conditions of material on fracture mechanisms. Fracture is thermodynamic structure-phase decomposition of a material, and hence development of nonlinear fracture waves is integrally linked with its initial structure-phase state and loading conditions. A thermodynamically stable material whose Gibbs thermodynamic potential is near the main minimum on the curve $F = F(v)$ (Fig. 1) has a high plasticity margin before the onset of structure-phase decomposition. A highly nonequilibrium material, e.g., a nanostructured material, is in thermodynamic proximity to structure-phase decomposition. It is not surprising that if bands with $F(v) > 0$ arise in a loaded nanostructured material, it experiences brittle fracture. However, the same material shows superplasticity, providing that the conditions $v < v_{cr}$ and $F(v) < 0$ are met during its deformation.

A more vivid example is brittleness of metallic glasses. Their amorphous structure is characterized

by $F(v) \sim 0$. Any nonlinear wave of local structural transformations provides the condition $F(v) > 0$ being responsible for structure-phase decomposition and brittle fracture of the material. In this respect, an extremely significant feature is the high plasticity of absolutely brittle materials, particularly minerals like marble, in a Bridgman anvil. Elimination of the conditions $v > v_{cr}$ and $F(v) > 0$ in a Bridgman anvil ensures high plasticity of any material. This suggests that an important role in fracture of material belongs to the principal normal stresses that control the variation in the molar volume and sign of the Gibbs thermodynamic potential in a deformed solid.

In the general case, fracture develops in the hierarchy of structural scales. Opening of a crack on the macroscale is a rotational deformation mode which must be accommodated by meso-, micro-, and nanoscale rotational modes. The character of this accommodation is governed by the normal to tangential stress ratio in the crack tip region. This ratio determines the type of cracks developing in a material: an opening mode crack, a sliding mode crack, or a tearing mode crack, each displaying its own form on a fracture surface. However on the nanoscale, whatever the case, the thermodynamic condition $v > v_{cr}$ and $F(v) > 0$ responsible for structure-phase decomposition of material in a fracture zone is bound to hold.

Multiscale fracture in a neck is described above in Sect. 2. Let us consider an example of fatigue fracture nucleating at the interface "plastically deformed surface layer – elastically loaded substrate" and developing as a typical nonlinear wave process [14].

The plastically deformed surface layer and the elastically loaded substrate were modeled by high-purity aluminum A999 foils glued on flat specimens of commercial aluminum or titanium and subjected to alternate bending. The foils were deformed plastically; the high-strength substrate was loaded elastically. After a certain number of loading cycles, the foils were unglued and cracking on its back side was studied with a laser profilometer.

At the first stage of cyclic loading, the back side of the foils revealed zigzag mesobands of localized deformation in the conjugate directions of maximum tangential stress τ_{max}. The zigzag propagation of mesobands is explained by chequered distribution of normal tensile and compressive stresses at the interface of two heterogeneous media [24]. According to [24], plastic shear under the action of tangential stress can develop only along squares of the chequered interface structure with an increased molar volume due to normal tensile stress. Further in the process, a fatigue crack develops along one of the mesobands of localized deformation, inheriting its zigzag character. The results under consideration allow the conclusion on the wave character of fatigue fracture in the two-layer composite.

The basis for the nonlinear fatigue fracture wave is two-scale self-consistency of localized shear attended by material rotations in the plastically deformed soft foil and localized shear-induced counter elastic displacements and rotations in the high-strength substrate. Figure 9(*a*) shows a displacement vector field ahead of the fatigue crack tip in the polycrystalline Al specimen obtained with a television-optical measuring complex [25]. The displacement vector field suggests a pattern of the stress-strain state in the zigzag mesoband during the propagation of a fatigue crack in it (Fig. 9(*b*)). The stress concentrator K at the crack tip generates maximum shear stresses in the mesoband along the directions **KC** and **KD** [20]. The vector sums **KC** = **KS** + **KE** and **KD** = **KS** + **KF** provide opening of the crack by the normal stresses **KE** and **KF** and its longitudinal propagation along the vector 2**KS**. Similar stress vector fields arise also at all links of the zigzag mesoband of localized shear.

The pattern of zigzag propagation of localized shear mesobands along the conjugate directions τ_{max} (Fig. 9(*b*)) provides opening of the zigzag fatigue crack in the Al foil under the conditions of elastic deformation of the high-strength substrate. Let us demonstrate that the propagation of the crack along the zigzag mesoband at the interface of the two-layer composite is a nonlinear wave process in the two-scale medium.

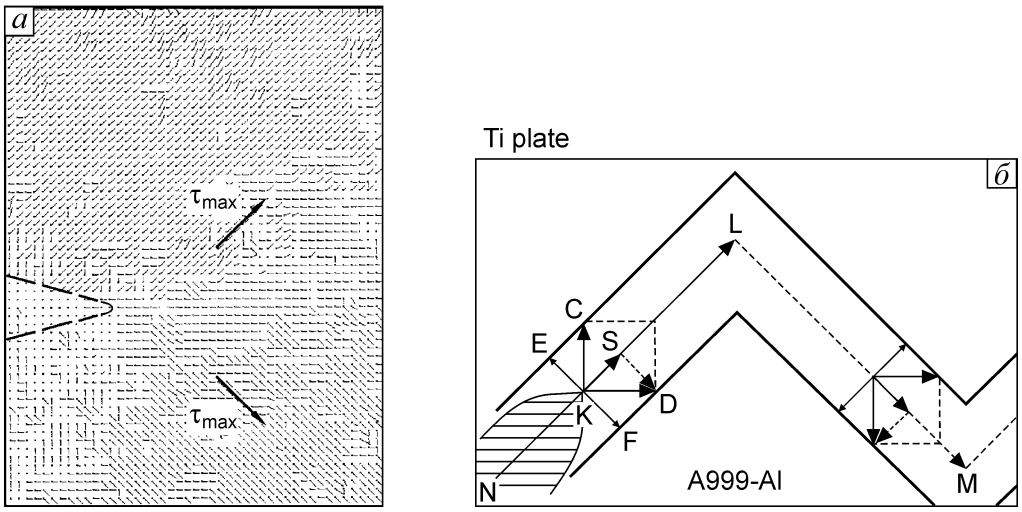

Fig. 9. Displacement vector field ahead of the fatigue crack, commercial Al, alternate bending, $N = 7.8 \cdot 10^6$ cycles, $T = 293$ K, $\times 100$ [25] (*a*); stress-strain scheme of fatigue crack *NK* propagation within mesoband *NLM* (*b*) [14].

Figure 10 presents mechanisms of local rotation in the region of the zigzag crack tip in the foil. In the single-scale approach, similar vortex plastic deformation at the tip of a fatigue crack is described in detail in [26]. It is easily seen in Fig. 10 that opening of the crack *KL* in the foil occurs through development of vortex plastic shear with attendant material rotations in the deformed foil (they are marked by arrows in Fig. 10). In the two-layer composite, the elastically loaded substrate generates counter shear-rotation stress fields. They retard the development of plastic shears in the foil and hence the propagation of the fatigue crack, being responsible for opening of the crack mainly by rotation in one direction and for asymmetry of the vortex displacement field and associated material rotations in the foil. However, the tension–compression cycling in the foil in alternate bending assists in partial relaxation of counter stress fields in the two-layer composite. This provides propagation of the zigzag plastic shear mesoband (and subsequent propagation of a crack in the band) at a distance *NN′*.

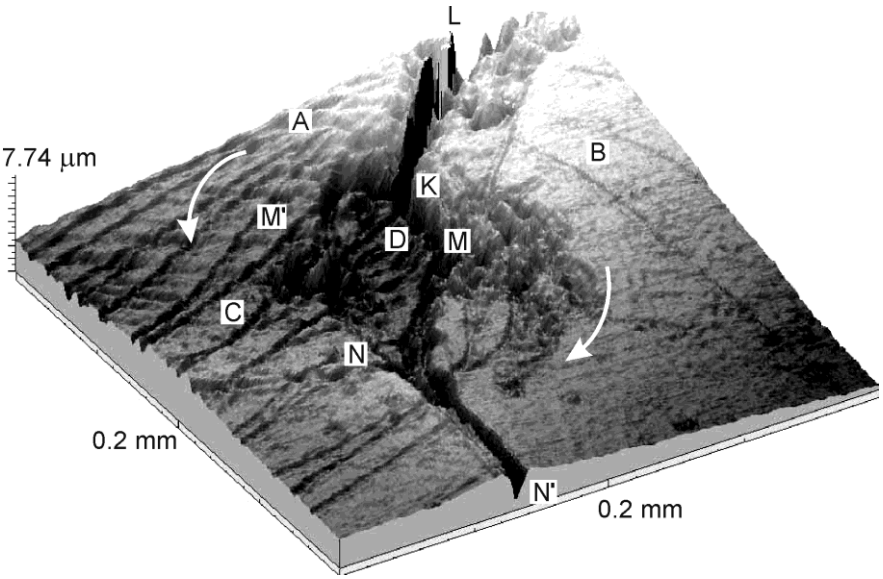

Fig. 10. Formation of the mesovortex *D* within zigzag crack, aluminum A999, alternate bending, $N = 2.5 \cdot 10^4$ cycles, $T = 293$ K [14].

At the same time, increasing the number of loading cycles causes a progressive growth of counter shear-rotation fields in the two-layer medium, and the defect material in the foil mesoband reaches its critical state. The plastically deformed material looses its shear stability, is fragmented, and the material rotation in the vortex structure of plastic shear ahead of the crack tip is transformed into a localized mesovortex *D* of crystallographic rotation (Fig. 10). The crack changes its trajectory in a jump-like manner and propagates further along the zigzag *NN′* in the conjugate direction τ_{max}. Thus, the zigzag character of fatigue crack propagation in the foil owes to the nonlinear wave nature of its propagation in the two-layer Al A999/Ti composite. Each zigzag of the crack reflects the damping factor during its propagation as a nonlinear wave in the blowup mode. The interaction of the rotational mode of the crack and the elastically loaded substrate in the two-layer composite gives rise to a rotational stress mesoconcentrator as an autocatalytic factor at the crack tip. This stress concentrator causes propagation of a new zigzag of the fatigue crack. The nonlinear wave process is repeated at each zigzag of the fatigue crack.

It is clearly seen at the lateral face of the unglued foil presented in Fig. 10 that an element of the crack zigzag *NN′* in the foil arises at the interface of the two-layer composite (in the zone *N′*) and then propagates throughout the foil thickness. This strongly supports the two-scale model of fatigue crack nucleation and propagation in a two-layer composite.

Notice that nucleation and propagation of a crack at the interface is associated with its channeling in the chequered distribution of normal tensile and compressive stresses. The crack can develop only with the availability of an excess molar volume. At the interface, the excess molar volume is in squares of normal tensile stress. Therefore, the zigzag crack trajectory in a multilayer medium is due to the chequered distribution of the excess molar volume at the interface of heterogeneous media. This governs the zigzag crack trajectory along the conjugate directions τ_{max} and underlines a fundamentally important role of couple forces in nonlinear wave propagation of the crack.

5. Wave propagation of an opening mode crack. Under cyclic loading when a specimen bulk is loaded elastically, the fatigue crack velocity in a plastically deformed surface layer is low. As the condition $v > v_{cr}$ in this type of fracture is attained due to normal tensile stress, a crack propagates under the action of tangential stress. This renders the tangential stress a decisive role in wave propagation of the crack and governs the formation of a sliding mode crack or a tearing mode crack. Fractographs of this fracture reveal a rather uniform roughness (Fig. 4(*a*, *b*)).

The authors of [27] demonstrated the wave character of fracture with a decisive contribution of normal tensile stress. In the work, the test specimens were commercial titanium with a submicrocrystalline structure and were in thermodynamic proximity to the condition $F(v) \sim 0$. In the bulk of a flat specimen of thickness 6 mm, a chevron notch was made such that the test specimen section was triangular (Fig. 11(*a*)). As the ends of the flat specimens were uniaxially stretched, a powerful stress concentrator with a characteristic highly stiff stress state arose at the notch tip *C*. This stress concentrator generated an opening mode crack that propagated in the chevron specimen with periodic arrests in the form of white transverse bands on the fracture surface (Fig. 11(*b*)). Scanning electron microscopy of high magnification showed that in these white transverse bands, fine folds of the material that experiences structure-phase decomposition in the region of the opening mode crack are accumulated (Fig. 11(*c*)). Apparently, the two-phase mixture of pores and nanostructured material is capable for viscous flow under the action of tangential stress at the crack front and accumulation in the form of white transverse bands on crack arrests on the fractograph. This corresponds to the damping factor of the nonlinear wave process of crack propagation. The crack arrest in the zone of white transverse bands corresponds to the autocatalytic factor of the nonlinear wave process. The autocatalytic factor is associated with recovery of the stress concentrator necessary for further crack propagation as a relaxation process.

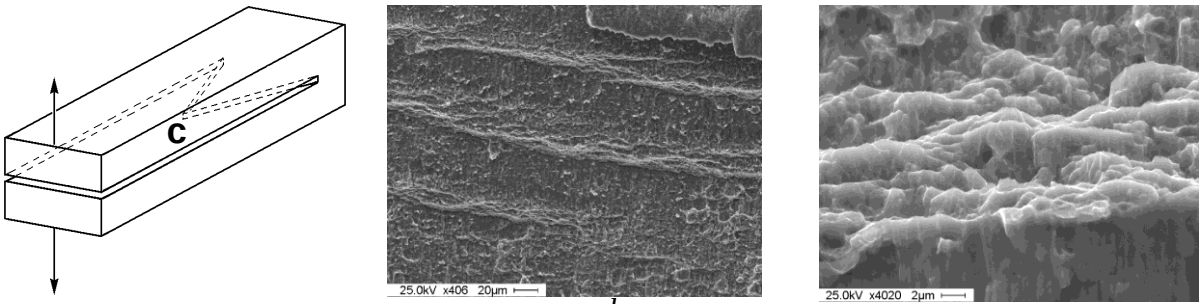

a *b* *c*

Fig. 11. Nonlinear wave of an open mode crack propagation: scheme of a chevron-notched tensile specimen (*a*); regular distribution of transverse white mesobands on the fracture surface of the submicrocrystalline commercial Ti, REM (*b*); fine substructure of a white transverse mesoband, REM (*c*) [27].

Nonlinear fracture waves are surely kinetic processes that depend on temperature and loading rate. These problems were studied in detail using the phenomenological approach by researchers of the St. Petersburg school [28, 29]. The available experimental regularities in the kinetic nature of strength of solids [30, 31, etc.] agree well with the nonlinear wave fracture theory presented in the paper.

Summary

In modern fracture mechanics, much attention is given to analysis of the stress-strain state in a local zone of material ahead of the crack tip. In the present paper, the concept was developed that crack nucleation in a stress concentrator zone meets the condition $v > v_{cr}$ under which the Gibbs thermodynamic potential becomes positive. A solid in these zones experiences local structure-phase decomposition. The thus arising crack propagates as a relaxation process in the stress concentrator gradient field. Further the crack is arrested and at its tip a new stress concentrator is formed under applied stress to provide structure-phase decomposition of the material ahead of the arrested crack. This mechanism of crack propagation develops as a nonlinear wave process. The nonlinear wave character of crack propagation is confirmed by experimental data.

A fundamentally important role in the wave process of crack propagation belongs to the condition $v > v_{cr}$ provided by normal tensile stresses. Tangential stresses determine the relaxation component of the wave process. The normal to tangential stress ratio in the nonlinear wave process of crack propagation determines the crack mode: opening, sliding, or tearing.

In the framework of gauge field theory of defects, the physical theory of crack propagation as a nonlinear wave process was proposed. The derived wave equations takes into account strains related to normal and tangential stresses. Particular attention was given to vorticity of defect flows due to generation of strain-induced defects in ductile fracture of material. This parameter is very important for analysis of roughness on fracture surface. The developed wave theory agrees well with available kinetic concepts of strength of solids.

The work was supported by projects of SB RAS Nos. III.20.1.1. and 72, Presidium of RAS Nos. 2.2 and 25.3, RFBR No. 10-01-13300-RT_omi and grant of the President of the Russian Federation for support of leading scientific schools No. NSh-6116.2012.1.

References

[1] *Fracture. A Topical Encyclopedia of Current Knowledge,* edited by G.P. Cherepanov (Krieger Publishing Company, Malabar, Florida 1998).

[2] *Abstract Book of the 11th Int. Conf. on Fracture,* edited by A. Carpinteri (Politecnico di

Torino, Italy 2005).
[3] G.C. Sih: Phys. Mesomech., Vol. 13, No. 5–6 (2010), p. 233.
[4] V.E. Panin, V.E. Egorushkin and A.V. Panin: Phys. Mesomech., Vol. 13, No. 5–6 (2010), p. 215.
[5] V.E. Panin, V.E. Egorushkin and A.V. Panin: Phys. Mesomech., Vol. 15, No. 1 (2012), p. 7 (in Russian).
[6] V.E. Panin and V.E. Egorushkin: Phys. Met. Metallogr., Vol. 110, No. 5 (2010), p. 464.
[7] V.E. Panin, Yu.V. Grinyaev, A.V. Panin and S.V. Panin, in: *Proc. 6th Int. Conf. for Mesomechanics*, Patras Univ. Press, Greece (2004).
[8] L.S. Derevyagina, V.E. Panin and A.I. Gordienko: Phys. Mesomech., Vol. 11, No. 1–2 (2008), p. 51.
[9] L.S. Derevyagina, V.E. Panin and A.I. Gordienko: Dokl. Phys., Vol. 434 (2010), p. 1.
[10] V.V. Rybin: *High Plastic Strains and Fracture of Metals* (Metallurgia, Moscow 1986) (in Russian).
[11] L.S. Derevyagina, V.E. Panin and A.I. Gordienko: Adv. Mater. Spec. Iss. No. 7 (2009), p. 83.
[12] K. Hellan: *Introduction to Fracture Mechanics* (McGraw-Hill, New York 1984).
[13] V.E. Panin and R.D. Strokatov, in: *Physical Mesomechanics of Heterogeneous Media and Computer Aided Design of Materials*, edited by V.E. Panin, Cambridge International Science Publishing (1998).
[14] V.E. Panin, T.F. Elsukova and Yu.F. Popkova: Dokl. Phys., Vol. 57, No. 3 (2012), p. 100.
[15] V.E. Egorushkin: Sov. Phys. J.,Vol. 33, No. 2 (1990).
[16] V.E. Egorushkin, in: *Physical Mesomechanics of Heterogeneous Media and Computer Aided Design of Materials*, edited by V.E. Panin, Cambridge International Science Publishing (1998).
[17] E. Kroner: *Gauge Field Theories of Defects in Solids* (Max Planck Inst., Stuttgart 1982).
[18] A. Kadič and D.G.B. Edelen: A Gauge Theory of Dislocations and Disclinations, in *Lecture Notes in Physics*, volume 174, Springer, Berlin (1983).
[19] S. Yoshida: Phys. Mesomech., Vol. 4, No. 3 (2001), p. 29.
[20] A.I. Mc Connel: *Application of Tensor-Analysis* (Dover Publ., New York 1957).
[21] V.E. Panin, N.S. Surikova, T.F. Elsukova, V.E. Egorushkin and Yu.I. Pochivalov: Phys. Mesomech., Vol. 13, No. 3–4 (2010), p. 103.
[22] V.E. Panin and V.E. Egorushkin: Phys. Mesomech., Vol. 14, No. 5–6 (2011), p. 207.
[23] N.S. Surikova: *Doctoral Degree Dissertation* (ISPMS SB RAS, Tomsk 2012) (in Russian).
[24] V.E. Panin, A.V. Panin and D.D. Moiseenko: Phys. Mesomech., Vol. 10, No. 1–2 (2007), p. 5.
[25] V.E. Panin, T.F. Elsukova and G.V. Angelova: Phys. Mesomech., Vol. 5, No. 3–4 (2002), p. 75.
[26] I. Botsis, in: *Fracture. A Topical Encyclopedia of Current Knowledge*, edited by G.P. Cherepanov, Krieger Publishing Company, Malabar, Florida (1998).
[27] E.E. Deryugin, V.E. Panin and L.S. Derevyagina, in: *Proc. ECF19*, Kasan, Russia (2012), in press.
[28] S.N. Zhurkov and Sanfirova: Physics of Solids, Vol. 2, No. 6 (1960), p. 1033.
[29] V.R. Regel, A.I. Slutsker and E.E. Tomashevsky: *Kinetic Nature of Strength of Solids* (Nauka, Moscow 1974) (in Russian).
[30] L.R. Botvina: *Fracture. Kinetics, Mechanisms, General Regularities* (Nauka, Moscow 2008) (in Russian).
[31] Yu.V. Petrov, A.A. Gruzdkov and V.A. Bratov: Phys. Mesomech., Vol. 15, No. 5–6 (2012), p. 15. (in Russian).